EUROPEAN ORGANIZATION FOR NUCLEAR RESEARCH
CERN - AB DIVISION

CLIC Note 557

Commissioning of a bunch frequency monitor for the CTF3 preliminary phase

A. Ferrari, A. Rydberg
Uppsala University, Sweden

F. Caspers, R. Corsini, L. Rinolfi, P. Royer, F. Tecker
CERN, Geneva, Switzerland

Abstract

The CTF3 preliminary phase at CERN has demonstrated the feasibility of the bunch frequency multiplication process, by injection of subsequent bunch trains into an isochronous ring. In order to observe the bunch interleaving at each stage of this process, a new method based on frequency spectrum analysis has been developed. For this purpose, a coaxial RF pick-up and its detection system were designed and mounted in the CTF3 ring, in order to allow comparison of the amplitudes of five harmonics of the fundamental beam frequency (9, 12, 15, 18 and 21 GHz) while combining bunch trains. The commissioning of this monitor was a successful proof of principle for this new method, however with two limitations: the short length of the bunch trains and the presence of parasitic signals associated with waveguide modes propagating with the beam inside the pipe.

February 28, 2003

1 Introduction

The Compact Linear Collider (CLIC) RF power source is based on a new scheme of bunch frequency multiplication, in which the drive beam time structure is obtained through the combination of electron bunch trains in isochronous rings, using RF deflectors [1]. The preliminary phase of the CLIC Test Facility CTF3 [2] has successfully demonstrated the feasibility of such a scheme at low charge [3, 4]. A pulse train consisting of up to five pulses, produced by the source at the front-end and accelerated in a linac, was injected into an isochronous ring by using RF deflectors which create a time-dependent closed bump of the reference orbit and thereby allow the interleaving of the pulses at the injection. Bunch frequency multiplication factors of four and five were demonstrated. In order to visualize the longitudinal structure of the pulses and to monitor the interleaving of bunches during the operation of the CTF3 preliminary phase, a streak camera was used. This device measures the synchrotron radiation produced by the electrons in a short bending magnet section of the ring. The structure of the light pulse can be related to that of the bunch trains. The streak camera was used to observe the beam over several turns in the ring and it clearly showed that electron pulse compression was occurring.

In this paper, we present an alternative method to monitor the bunch train combination, based on frequency spectrum analysis. When the first pulse is injected into the isochronous ring, the distance between two consecutive bunches is 10 cm, i.e. 333 ps. Therefore, all harmonics of 3 GHz can be found in the beam power spectrum. At the end of the bunch train combination, the distance between two consecutive bunches is reduced by a factor of four or five and, as a result, only the harmonics of respectively 12 or 15 GHz should be found in the beam power spectrum. More details on this issue can be found in Section 2 where the effect of some systematic errors on the beam frequency spectrum measurement are also studied. In Section 3, we study the response of the coaxial pick-up used to extract the information contained in the beam. In Section 4, we describe the instrumentation used to analyse the signals coming out from the pick-up and we report on calibration tests. In September and October 2002, the so-called Uppsala bunch frequency monitor was installed and commissioned at CERN during the last operating period of the CTF3 preliminary phase: a description of the measurements that were performed, as well as an analysis of the results that were obtained, are given in Section 5. Finally, conclusions are drawn in Section 6.

2 Beam frequency spectrum calculations

2.1 Electromagnetic field induced by an electron bunch

Let us consider a bunch of N ultra-relativistic electrons following a straight trajectory in free space. We assume that it has a gaussian longitudinal charge distribution $\Lambda(z)$:

$$\Lambda(z) = \frac{1}{\sqrt{2\pi}\sigma_z} exp\left(-\frac{z^2}{2\sigma_z^2}\right).$$

In cylindrical coordinates, the transverse fields which are excited by the beam have the following form:

- $H_\theta(r,t) = \frac{Ne}{2\pi r} \times \frac{1}{\sqrt{2\pi}\sigma_t} exp\left(-\frac{t^2}{2\sigma_t^2}\right)$,
- $E_r(r,z) = Z_0 \times H_\theta(r,z)$ with $Z_0 = \sqrt{\mu_0/\epsilon_0}$.

For the CTF3 preliminary phase, the nominal bunch length σ_t is 10 ps fwhm, i.e. 4.25 ps rms, and the nominal charge per bunch is 0.1 nC.

2.2 Calculation of the beam power spectrum

The electromagnetic power induced by a single bunch on the beam pipe is proportional to the square of the modulus of the Fourier transform of the (gaussian) longitudinal charge distribution of this bunch:

$$P_{bunch}(f) \propto exp(-4\pi^2 f^2 \sigma_t^2).$$

Let us now consider a train of N_b bunches which all have the same charge distribution $\Lambda(z)$. The time distribution of this train is the convolution of the field for one single bunch with a train of Dirac pulses. Its Fourier transform is thus a sum of pulses:

$$(\vec{E};\vec{H})_{train} = (\vec{E};\vec{H})_{bunch} \otimes \sum_{i=1}^{N_b} \delta(t-\tau_i),$$

$$F_{train}(f) = F_{bunch}(f) \times \sum_{i=1}^{N_b} exp(-j2\pi f \tau_i).$$

Therefore, the power spectrum of a train of electron bunches can be written as:

$$P_{train}(f) \propto exp(-4\pi^2 f^2 \sigma_t^2) \times \left[\left(\sum_{i=1}^{N_b} cos(2\pi f \tau_i) \right)^2 + \left(\sum_{i=1}^{N_b} sin(2\pi f \tau_i) \right)^2 \right].$$

In the CTF3 preliminary phase, each pulse consists of 20 electron bunches spaced by 10 cm, i.e. 333 ps. The distance between two consecutive pulses corresponds to the isochronous ring circumference, i.e. 420 ns. Indeed, the bunch train combination requires $C = n\lambda_0 \pm \lambda_0/N$, where n is an integer, C is the ring circumference, N is the combination factor and λ_0 is the RF wavelength [2]. Bunch frequency multiplication factors of four and five are considered in the following.

The first plot of Figure 1 and Figure 2 shows the normalized power spectrum for a train of 20 identical bunches, which have a fwhm length of 10 ps and which are spaced by 10 cm. The distance between two consecutive lines is thus 3 GHz. The envelope shown as a dashed line corresponds to the spectrum of a single bunch with the same rms length as the individual bunches of the train. The last plot of Figure 1 (respectively Figure 2) shows the normalized power spectrum at the end of the bunch frequency multiplication

process, with a factor four (respectively five): the final pulse consists of 80 bunches spaced by 2.5 cm (respectively 100 bunches spaced by 2 cm). The distance between two consecutive lines is now 12 GHz (respectively 15 GHz) and the envelope remains the same. The evolution of the normalized power spectrum when injecting the intermediate bunch trains in the isochronous ring is also shown in both Figure 1 and Figure 2.

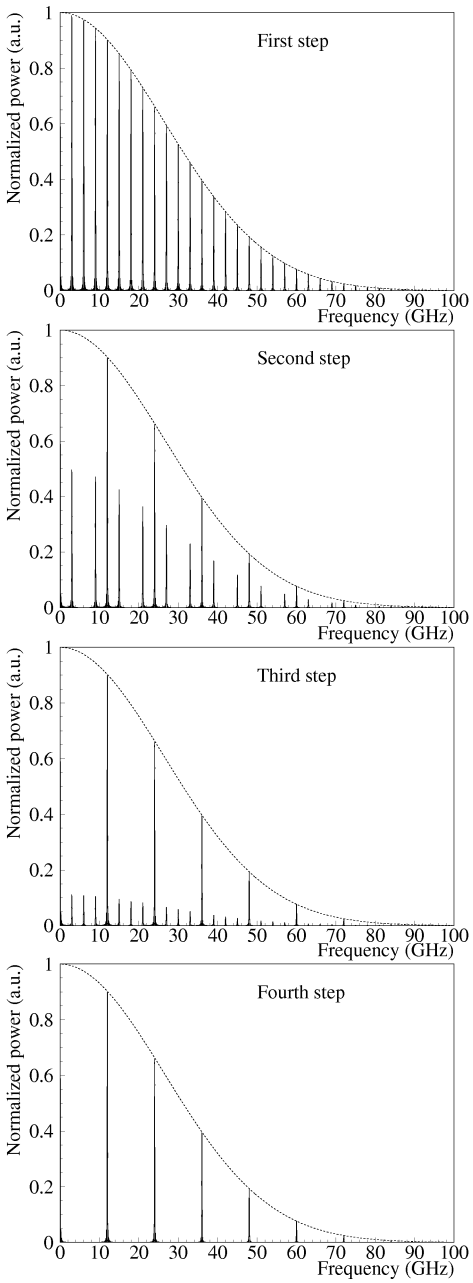

Figure 1: Normalized power spectra for a train of electron bunches with a fwhm length of 10 ps at various stages of the bunch frequency multiplication process with a factor four.

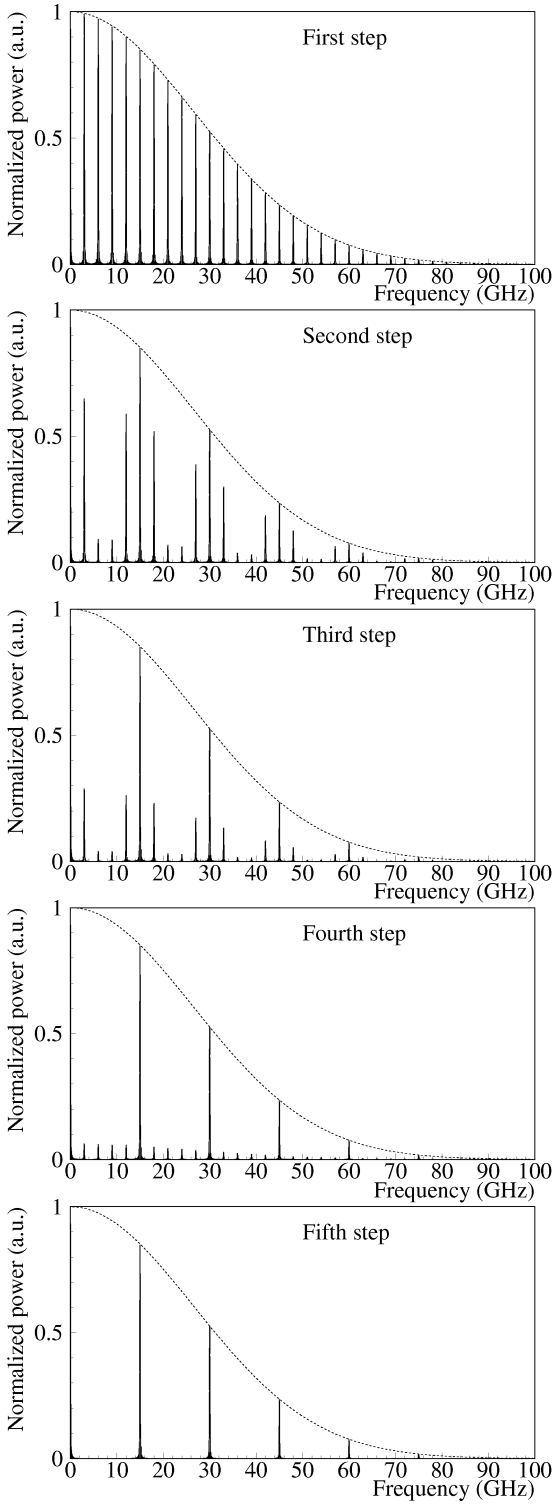

Figure 2: Same as Figure 1 but we now consider a bunch frequency multiplication with a factor five.

In the following part of this report, we focus on the systematic errors that can influence the distribution of power between the various harmonics of the beam spectrum. For this purpose, we only consider the case of a bunch frequency multiplication with a factor five, being aware that very similar results can be obtained with a factor four. For the sake of simplicity, we assume that the bunch length σ_t is constant over the whole bunch train.

2.3 Influence of bunch to bunch signal amplitude variations

If we assume that the longitudinal charge distribution is the same for all bunches, then the amplitude of the transverse fields excited by the bunch i only depends on its charge q_i and on the distance r_i between the bunch and a sensitive device installed on the beam pipe wall. As a result, the power spectrum of a bunch train can be rewritten as:

$$P_{train}(f) \propto exp(-4\pi^2 f^2 \sigma_t^2) \times \left[\left(\sum_{i=1}^{N_b} a_i \, cos(2\pi f \tau_i) \right)^2 + \left(\sum_{i=1}^{N_b} a_i \, sin(2\pi f \tau_i) \right)^2 \right],$$

where the signal amplitude a_i depends on q_i and r_i.

In a first step, the values of a_i were randomly chosen between $0.5\,a_0$ and $1.5\,a_0$, where a_0 is the signal amplitude that one would obtain with a train of identical bunches. No significant effect was observed in the normalized power spectrum at each step of the bunch train combination process, when compared to the nominal case of Figure 2.

Let us now introduce systematic amplitude variations. For this purpose, we assume that the charge per bunch and the distance between the beam and the vacuum pipe wall is constant over one bunch train, but that they can vary from one bunch train to the other. If f is an harmonic of 3 GHz, the terms $a_i \, cos(2\pi f \tau_i)$ and $a_i \, sin(2\pi f \tau_i)$ are identical for all bunches in the same train. If N_p is the number of bunch trains in the ring, the power spectrum can now be derived from:

$$P_{train}(f) \propto exp(-4\pi^2 f^2 \sigma_t^2) \times \left[\left(\sum_{j=1}^{N_p} a_j \, cos(2\pi f \tau_j) \right)^2 + \left(\sum_{j=1}^{N_p} a_j \, sin(2\pi f \tau_j) \right)^2 \right].$$

Let us assume that $a_j = a_0\,(1 + \epsilon_j)$. Figure 3 shows the evolution of the normalized power spectrum at each step of the bunch frequency multiplication process with a factor five. Here, $\epsilon_1 = 0$, $\epsilon_2 = -0.50$, $\epsilon_3 = +0.25$, $\epsilon_4 = -0.25$ and $\epsilon_5 = +0.50$.

At the end of the bunch train combination, most of the power is shared between the harmonics of 15 GHz, as in the nominal case. However, the evolution of the beam power spectrum during the bunch frequency multiplication process significantly depends on the train to train variation of the transverse field amplitude. After some algebra, we can show that, for the harmonics of 15 GHz, the normalized power is easily calculated with:

$$P_{15}(N_p) = P_{nominal} \times (1 + \tilde{\epsilon}) \text{ where } \tilde{\epsilon} = \frac{1}{N_p} \sum_{j=1}^{N_p} \epsilon_j.$$

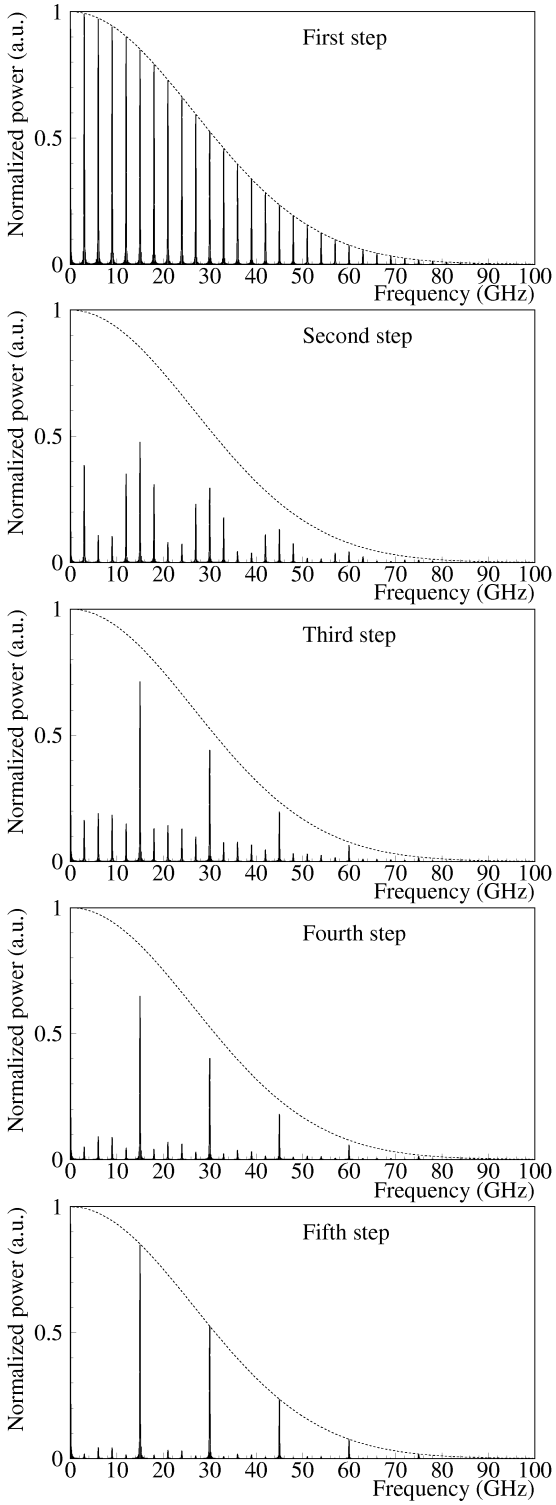

Figure 3: Same as Figure 2 but we have introduced systematic variations of the transverse field amplitude from one bunch train to the other (see text for details).

2.4 Influence of bunch phase errors

Let us now consider a train in which all bunches are identical. If the bunch frequency multiplication (with a factor five) works well, then the distance between the bunches injected at the stage j and the bunches injected at the stage $j+1$ is exactly $\tau/5$, where $\tau = 333$ ps. However, if a systematic phase error occurs at injection, then one should replace $\tau/5$ by $\tau/5+\phi$. The phase shift ϕ has a significant effect on the amplitude of the harmonics found in the power spectrum. If there was no phase error at injection, only the harmonics of 15 GHz would be present in the frequency spectrum at the end of the bunch combination process. But, because of the systematic phase error, some harmonics of 3 GHz, which are not harmonics of 15 GHz, are still found in the power spectrum at the end of the bunch train combination process.

In the following, we focus on five frequencies, namely 9, 12, 15, 18 and 21 GHz. The power associated with each of these harmonics has been calculated for various values of the phase error, see Figure 4. The larger the phase error, the smaller the power associated with the 15 GHz harmonic, and the larger the power associated with some harmonics of 3 GHz which are not harmonics of 15 GHz. In particular, when the spacing between the bunches injected at the stage j and the bunches injected at the stage $j+1$ is larger than $\tau/5$, the bunch frequency multiplication factor is between 4 and 5, therefore the 12 GHz harmonic also receives power. Similarly, when the spacing between the bunches injected at the stage j and the bunches injected at the stage $j+1$ is smaller than $\tau/5$, the bunch frequency multiplication factor is between 5 and 6, and some power goes into the 18 GHz harmonic.

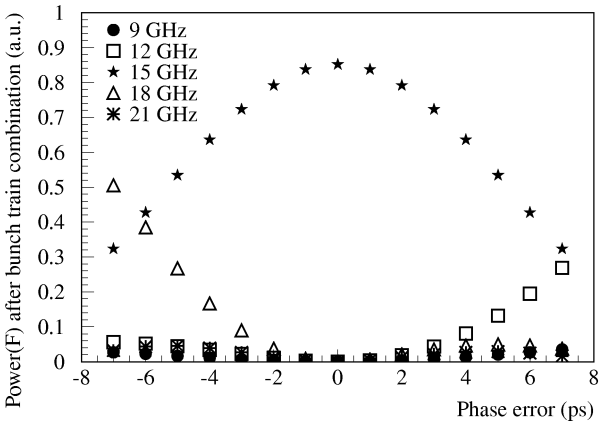

Figure 4: Power (in arbitrary units) associated with the harmonics at 9, 12, 15, 18 and 21 GHz at the end of the bunch frequency multiplication, as a function of the phase error.

Note that, since the 3 GHz intrinsic structure of each bunch train is not affected by the phase shift, the positions of the lines in the power spectrum remain unchanged, and new harmonics at frequencies other than the multiples of 3 GHz are not observed.

3 Simulation of the coaxial pick-up

In this section, we discuss the performance of the coaxial RF pick-up used to extract the information contained in the bunch trains. The electromagnetic fields excited in the pick-up by the passage of a bunch through the beam pipe can be calculated by solving Maxwell's equations numerically with MAFIA [5]. This program computes the amplitude of the modes which propagate along the pick-up (in MAFIA, the amplitude of a mode is defined as the square root of the associated electromagnetic power).

In the very first design of the pick-up, the signals were extracted through a 50 Ω coaxial line having an inner diameter of 0.4 mm and an outer diameter of 0.92 mm [6]. This geometry was chosen in order to make sure that only a TEM mode propagates in the pick-up and that the high-order TE and TM waveguide modes are evanescent in the frequency range of interest (between 9 and 21 GHz). Then, the design of the pick-up evolved in order to include a miniature ultrahigh vacuum feedthrough [7] while meeting various technical constraints. The final geometry of the pick-up is shown in Figures 5 and 6. The feedthrough can be considered as a two dielectric coaxial line, for which an adaptation to 50 Ω can be achieved over more than half of its length. The inner conductor has a constant diameter of 0.4 mm. On the vacuum side, it is maintained in its central position by a small ceramic ring. A hole with a diameter of 1.5 mm was drilled in the beam pipe wall for the extraction of the signal. On the other side, the feedthrough is terminated by a K connector, which can be considered as a 50 Ω coaxial line filled with a dielectric made of air and kapton (the diameters of the inner and outer conductors are respectively 0.9 mm and 2.5 mm).

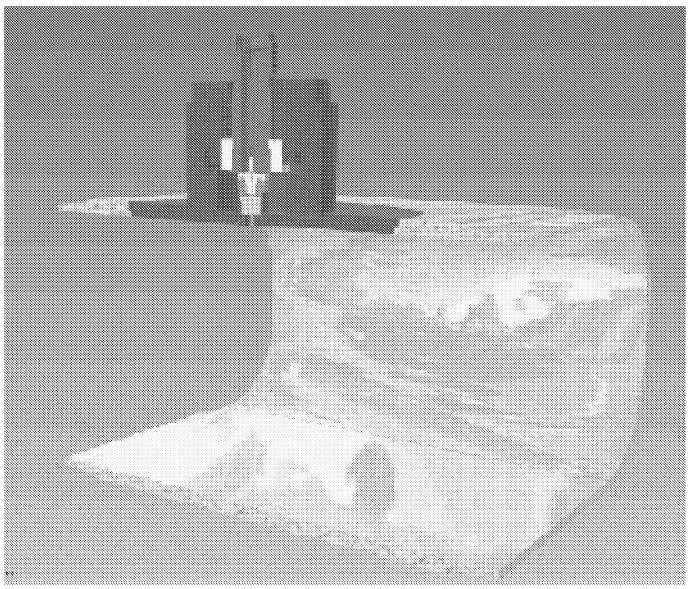

Figure 5: Three-dimensional cross-section view of the coaxial RF pick-up installed on the beam pipe of the CTF3 ring.

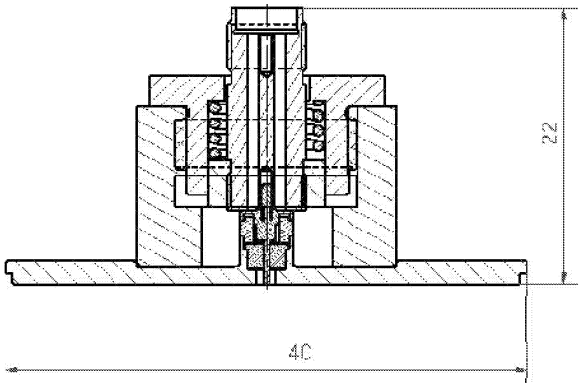

Figure 6: Technical drawing of the coaxial RF pick-up (the dimensions are in mm).

3.1 Estimation of the pick-up response

The geometry of the coaxial pick-up was included in the MAFIA simulations. Then, we computed the signal at the output of the RF pick-up when one gaussian bunch with a charge of 0.1 nC and a fwhm length of 10 ps travels on a straight trajectory at the center of the beam pipe. Finally, the transfer impedance Z_{tr} was determined by calculating the ratio between the Fourier transform of the output voltage and the Fourier transform of the beam current I_b. Table 1 shows the values of Z_{tr} that were computed for the five frequencies of interest.

Frequency (GHz)	9	12	15	18	21
$Z_{tr}(\Omega)$	0.085	0.131	0.122	0.110	0.141

Table 1: Transfer impedance of the coaxial RF pick-up for the five frequencies of interest.

In the CTF3 preliminary phase, one pulse consists of 20 bunches spaced by 333 ps when injected into the isochronous ring. After the bunch frequency multiplication with a factor four or five, one obtains respectively 80 bunches spaced by 83 ps or 100 bunches spaced by 67 ps. Therefore, the time response of the pick-up is the convolution of the time response for one single bunch with a train of Dirac pulses. The power spectrum at the coaxial pick-up output can thus be calculated as follows:

$$P(f) = \left(\frac{|Z_{tr}(f)| \times I_b(f)}{\sqrt{R}} \right)^2 \times \left[\left(\sum_{i=1}^{N_b} cos(2\pi f \tau_i) \right)^2 + \left(\sum_{i=1}^{N_b} sin(2\pi f \tau_i) \right)^2 \right],$$

where $R = 50\ \Omega$ is the output impedance of the pick-up, N_b is the number of bunches in the train and τ_i is the position of the bunch i in the train.

Figure 7 shows the power spectrum induced by one train of 20 bunches spaced by 333 ps at the pick-up output in the 8 - 22 GHz frequency range.

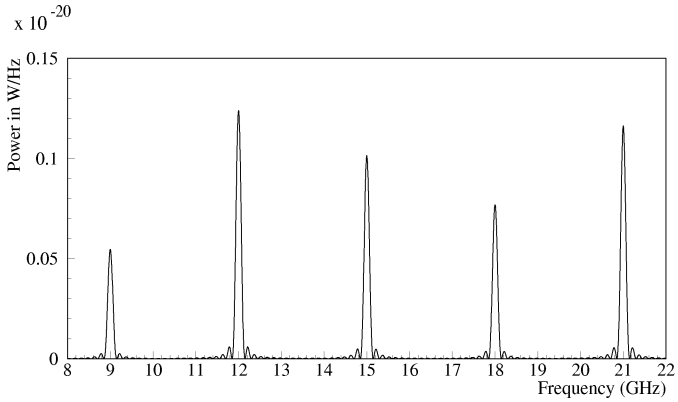

Figure 7: Power spectrum at the pick-up output for the 8 - 22 GHz frequency range, when a train of 20 bunches spaced by 333 ps travels at the center of the beam pipe.

Let $\delta t = 6.6$ ns be the length of the bunch train. Each of the peaks in the power spectrum can be expressed as follows:

$$P_i(f) = A_i^2 \times \left(\frac{sin\pi\delta t[f - f_i]}{\pi\delta t[f - f_i]} \right)^2 .$$

When taking the inverse Fourier transform of $\sqrt{P_i(f)}$, one obtains:

$$\sqrt{P_i(t)} = \frac{A_i}{\delta t} \times exp(j2\pi f_i t) \text{ if } |t| < \frac{\delta t}{2}, 0 \text{ otherwise.}$$

The signal at the pick-up output is a superposition of pulses with a length $\delta t = 6.6$ ns and a mode amplitude $A_i/\delta t$, oscillating at a frequency f_i. For each harmonic of interest, Table 2 and Table 3 give the power in the pulse coming out from the pick-up, at each stage of the bunch frequency multiplication, with respectively a factor four or five.

Step	Power for each harmonic f_i			
	9 GHz	12 GHz	15 GHz	18 GHz
1	12.5 μW -19.0 dBm	28.5 μW -15.4 dBm	22.9 μW -16.4 dBm	17.6 μW -17.5 dBm
2	25.0 μW -16.0 dBm	114.0 μW -9.4 dBm	45.8 μW -13.4 dBm	0 μW –
3	12.5 μW -19.0 dBm	256.5 μW -5.9 dBm	22.9 μW -16.4 dBm	17.6 μW -17.5 dBm
4	0 μW –	456.0 μW -3.4 dBm	0 μW –	0 μW –

Table 2: Power in the pulse at the coaxial pick-up output for each harmonic of interest, at various steps of the bunch frequency multiplication with a factor four.

Step	Power for each harmonic f_i				
	9 GHz	12 GHz	15 GHz	18 GHz	21 GHz
1	12.5 μW −19.0 dBm	28.5 μW −15.4 dBm	22.9 μW −16.4 dBm	17.6 μW −17.5 dBm	26.4 μW −15.8 dBm
2	4.8 μW −23.2 dBm	74.6 μW −11.2 dBm	91.6 μW −10.4 dBm	46.1 μW −13.3 dBm	10.1 μW −20.0 dBm
3	4.8 μW −23.2 dBm	74.6 μW −11.2 dBm	206.1 μW −6.9 dBm	46.1 μW −13.3 dBm	10.1 μW −20.0 dBm
4	12.5 μW −19.0 dBm	28.5 μW −15.4 dBm	366.4 μW −4.4 dBm	17.6 μW −17.5 dBm	26.4 μW −15.8 dBm
5	0 μW −	0 μW −	572.5 μW −2.4 dBm	0 μW −	0 μW −

Table 3: Power in the pulse at the coaxial pick-up output for each harmonic of interest, at various steps of the bunch frequency multiplication with a factor five.

3.2 Pick-up response vs beam parameters

3.2.1 Pick-up response vs bunch properties

So far, we have only considered electron bunches with a charge $q_0 = 0.1$ nC and a fwhm length $\sigma_0 = 10$ ps. Here, other values of the bunch charge and length have been studied as well. For the sake of simplicity, we assume that the beam travels at the center of the beam pipe. Figure 8 shows how the power coming from the coaxial pick-up depends on the charge and the length of the bunches producing the excitation.

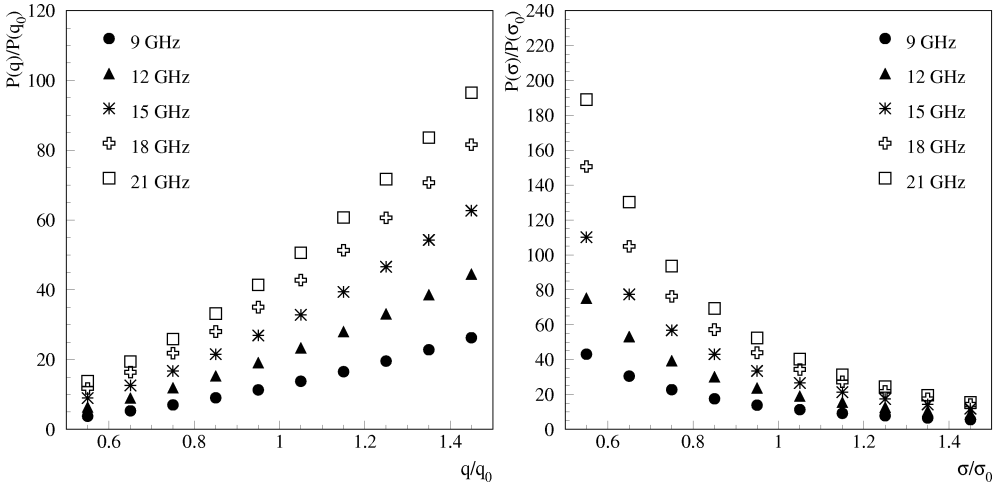

Figure 8: Variation of the power (expressed in μW) coming from the pick-up with the bunch charge (left) and the bunch length (right), for each harmonic of interest, before the bunch train combination (20 bunches spaced by 333 ps).

The ratios between the powers associated with different harmonics do not depend on the bunch charge, but they do depend on the bunch length. Note that the bunch properties (charge and length) only affect the beam current I_b, and not the transfer impedance Z_{tr}.

3.2.2 Pick-up response vs beam position

The transfer impedance of the system consisting of the beam pipe and of the pick-up is related to the position of the bunches in the tube. An off-center beam does not produce the same excitations as a beam passing exactly at the center of the tube, even if the current I_b is unchanged. Several simulations were thus performed in order to determine how the power of each harmonic of interest changes when the beam does not travel at the center of the tube.

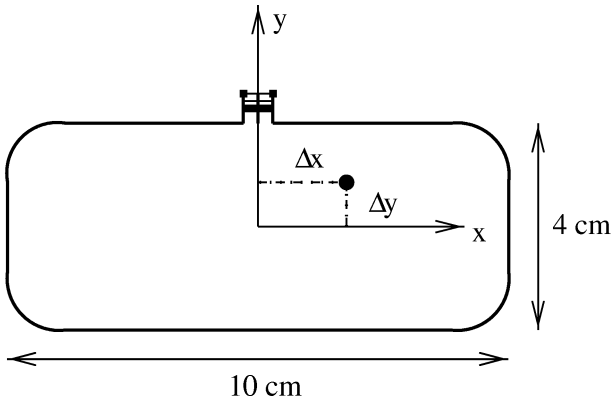

Figure 9: Off-center electron bunch in the beam pipe of the isochronous ring.

Figure 10 shows that, as in the case of bunch charge variations, the ratios between the powers associated to different harmonics do not depend on the transverse position of the beam in the tube.

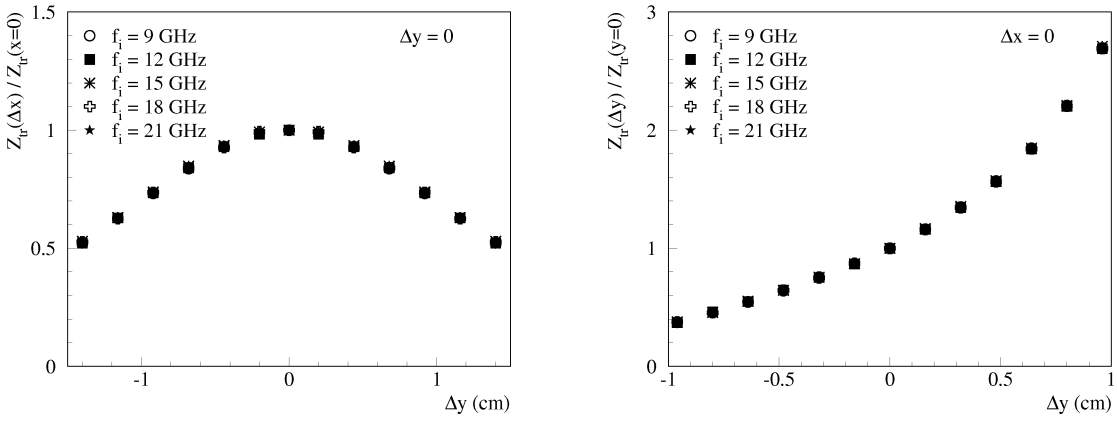

Figure 10: Variation of transfer function Z_{tr} with the transverse position of the beam.

In this study, the electron bunches do not have any transverse dimension and the beam is thus treated as a one-dimensional current in MAFIA: the contribution of the betatron oscillations is therefore neglected.

4 Calibration of the detection system

The RF pick-up signal is a superposition of pulses, at various frequencies f_i and with various amplitudes A_i. It is transported to the detection system through a 2 m long 50 Ω low loss SMA cable. There, the signal first goes through a wideband amplifier and a 10 dB attenuator. Afterwards, it travels along a second 50 Ω low loss SMA cable, with a length of 3 m. When re-entering the detection system box, the signal is divided into five channels, by using two power splitters. Each of these channels is terminated by a bandpass filter, in order to select the harmonic of interest (the signals having the wrong frequency are reflected, go through the 3 m SMA cable and are eventually damped in the 10 dB attenuator). For the filter at 21 GHz, the bandwidth at 3 dB is 2.1 GHz. For the four other channels, the bandwidth is 1 GHz. After the bandpass filter, each signal is sent through a low noise amplifier. Two types of amplifiers are used. For the channels corresponding to 9, 12, 15 and 18 GHz, the bandwidth at 3 dB is 6 - 18 GHz, and the maximum gain is 30 dB. For the harmonic at 21 GHz, the bandwidth at 3 dB is 18 - 26 GHz, and the maximum gain is 20 dB. Each detection line is terminated by a detector diode, which is aimed at measuring the amplitude of the incoming RF signal. The output signals are extracted from the detection system through SMA-BNC connectors, which then allow their transfer to an oscilloscope for further analysis. A general layout of the detection system is shown in Figure 11.

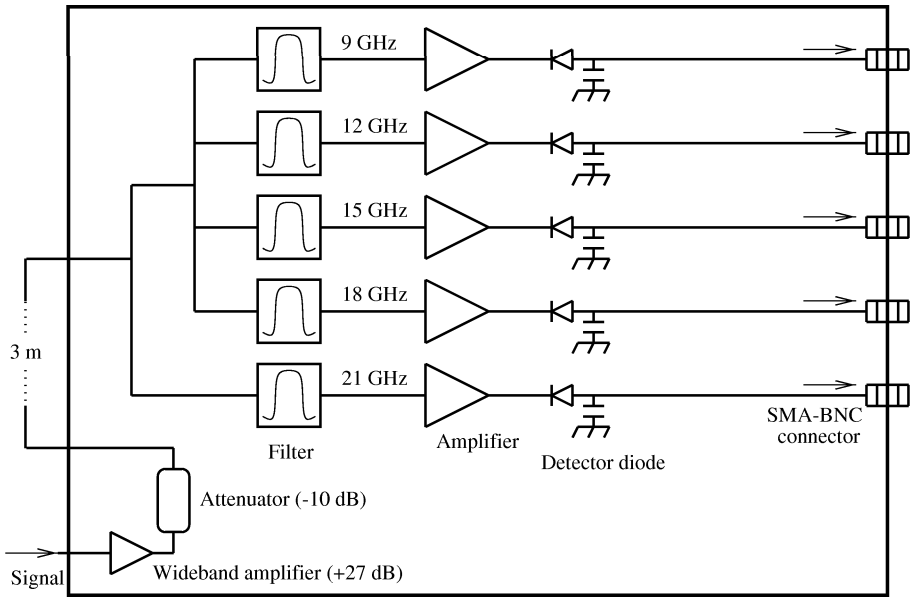

Figure 11: Schematic layout of the full detection system.

When assembling the detection system at Uppsala University, some measurements were performed with a network analyzer in order to determine the frequency response of each of the five channels, see Figure 12. For these measurements, the common input port is the extremity of the 2 m long SMA cable which is connected to the RF pick-up, and the output ports are located just upstream each of detector diode. We noticed that, for the filters in the 9 and 12 GHz channels, the rejection efficiency for the signals with a frequency larger than 20 GHz was rather poor. However, since the bandwidth of the amplifier placed just downstream of the filter is 6 - 18 GHz, the residual signal at high frequency remains very small (at least 20 dB lower than the signal of interest) and it can thus be neglected in the following. The response of the detector diode was also studied: by using an RF synthetizer in the sweep mode, we checked that there is no variation of the diode response with the input frequency.

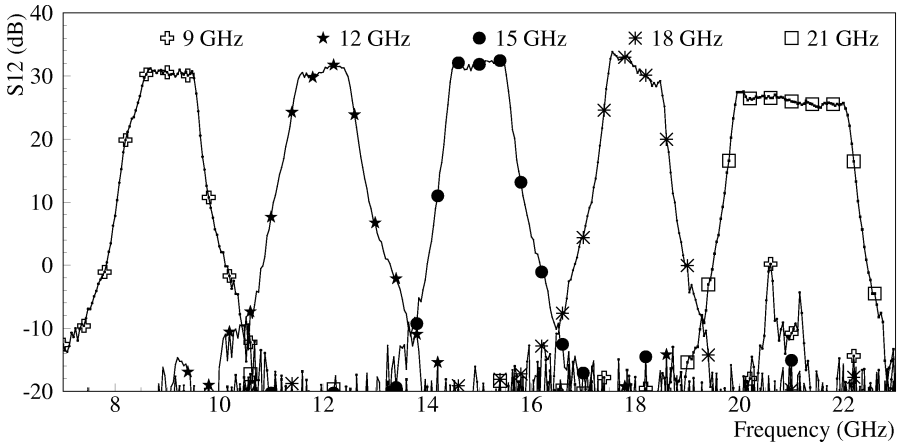

Figure 12: Transmission coefficient S12 as a function of the frequency for the five channels of the detection system, as measured between the input of the 2 m long SMA cable and the amplifier outputs.

The RF pick-up and the detection system were installed at CERN in September 2002. In order to avoid possible multiple reflections between the RF pick-up, which has a very high impedance, and the detection system, a 6 dB attenuator was mounted between the 2 m SMA cable and the instrumentation input, just upstream of the wideband amplifier. Downstream of the SMA-BNC connectors, the output signals are transported to the CTF3 control room through five 120 m long cables, where they are measured on a fast multi-channel digital oscilloscope. Before starting measurements with beam, calibration tests were performed in order to determine the amplitude response of the whole system (from the RF pick-up output to the oscilloscope) at each frequency of interest, see Figure 13. The detection system allows a large range of input powers to be covered (from -30 dBm up to 0 dBm). During these calibration tests, we noticed a failure in the 21 GHz channel: the amplifier had a leakage current which induced an offset voltage of -10 mV at the corresponding detection system output. Also, we observed a transition in the behaviour of the detector diode, when the input power is close to -5 dBm.

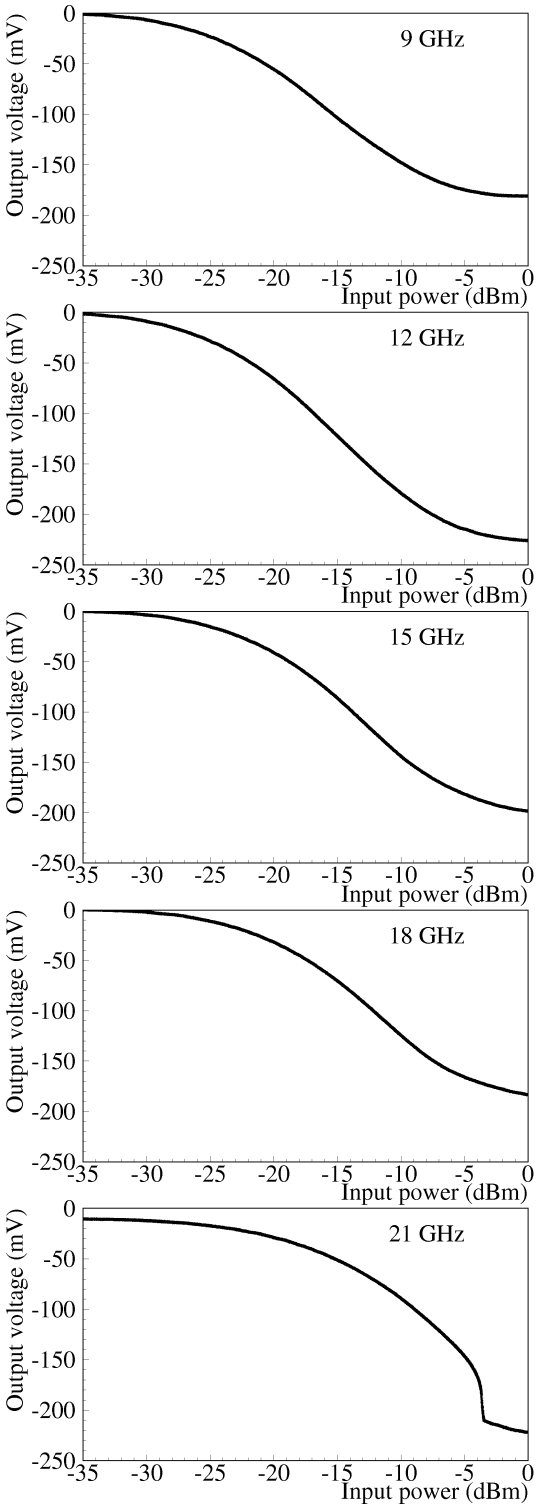

Figure 13: Amplitude calibration of the whole detection system (from the RF pick-up output to the fast digital multi-channel oscilloscope) at the five frequencies of interest.

Very long RF signals were sent into the detection system when measuring the calibration curves of Figure 13. However, the pulses coming from the coaxial RF pick-up are likely to be very short (about 6.6 ns). By driving an RF synthetizer operating at a fixed frequency with a DC pulse generator, we controlled the length of the RF signals that were injected into the detection system and we then noticed that the amplitude of the output signal on the oscilloscope was strongly dependent on the length of the RF pulse at the input of the detection system. In particular, if the length of the input RF pulse is of the order of a few ns, the detection system does not reach a steady state and the peak amplitude of the output signal is smaller than what it would be with a long input RF pulse. This is illustrated in Figure 14, which shows the response of the 15 GHz channel to two input RF pulses with the same amplitude of -15 dBm and with two different lengths.

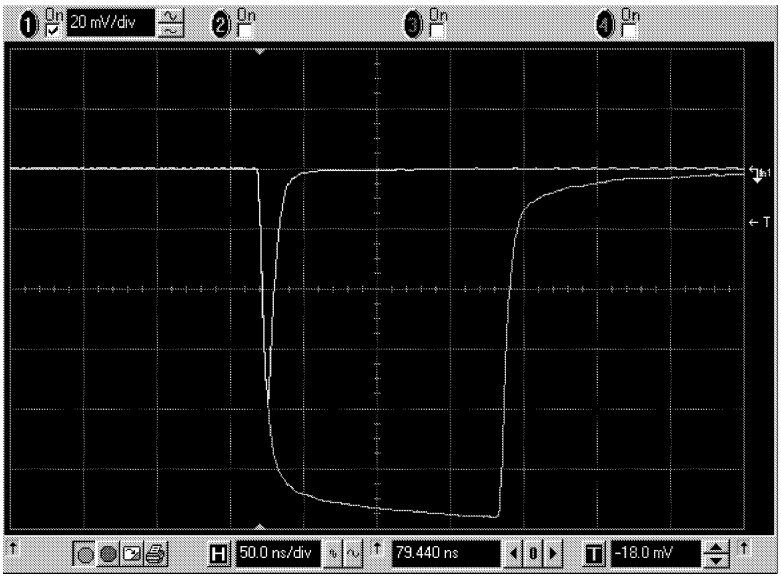

Figure 14: Response of the 15 GHz channel to RF pulses with the same amplitude of -15 dBm and with two different lengths: the short pulse is less than 10 ns long, while the long pulse is about 150 ns long. The fall time and the rise time of the measured signals are the same in both cases. No reflections are observed.

The short length of the electron bunch trains is one major limitation for the commissioning of the bunch frequency monitor during the operation of the CTF3 preliminary phase, since it does not allow a direct measurement of the amplitude of the signals coming out from the RF pick-up. An accurate calibration of the detection system is therefore difficult, because of the uncertainties related to the shape and the length of the bunch trains circulating in the CTF3 isochronous ring. However, in the future stages of the CTF3 project, the expected length for the electron bunch trains is 140 ns. The measurement of the power coming from the RF pick-up will then be much easier, since the detection system can reach a steady state.

5 Commissioning with beam at CERN

The RF pick-up was installed in the CTF3 isochronous ring in September 2002, at the exit of the so-called HR.BHZ58 bending magnet, i.e. at the beginning of the long straight section used for injection. There, the dispersion is expected to be zero. The horizontal and vertical β-functions are expected to be 26.1 m and 7.2 m respectively, while the normalized rms emittance is about 15 π mm.mrad in both transverse directions. The beam energy measured in the ring is 337 MeV [8].

Two series of measurements were performed in October 2002. A 2 m long low loss cable terminated with a 6 dB attenuator was connected to the SMA output of the RF pick-up in order to extract the signal. It could then be either transported directly to the CTF3 streak camera laboratory for time domain measurements with a 20 GHz sampling oscilloscope, or filtered in the detection system and then transported to the CTF3 control room for further analysis in the frequency domain, see Figure 15.

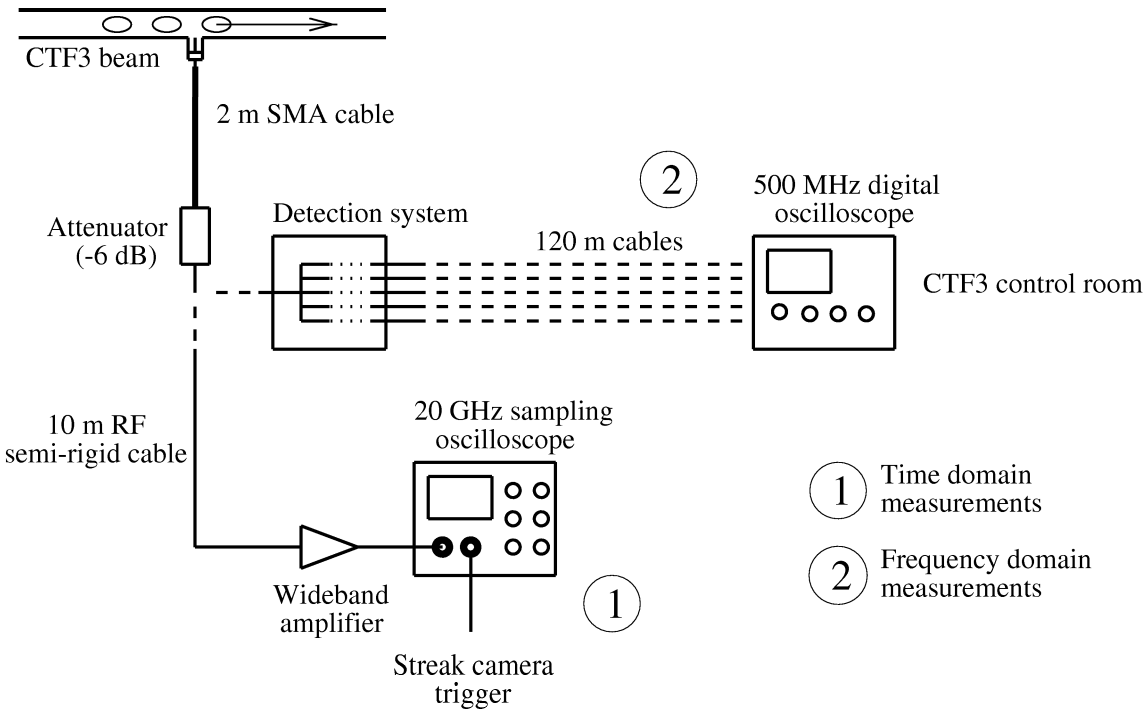

Figure 15: Installation of the Uppsala bunch frequency monitor in the CTF3 complex.

5.1 Time domain measurements

In order to visualize directly the time structure of the bunch trains circulating in the isochronous ring, the signals from the pick-up were transported to the CTF3 streak camera laboratory through a 50 Ω RF cable, with a total length of 10 m. There, the

signals were read on the sampling oscilloscope, triggered by the streak camera timing system. In order to cope with the losses along the cables and in the 6 dB attenuator installed downstream of the pick-up, a 27 dB wideband amplifier was mounted just upstream of the sampling oscilloscope.

In a first step, no bunch train combination was performed and the time structure of a single pulse was studied. Figure 16 shows that not only the signal produced by the 6-7 ns long bunch train is detected. Some reflections may occur in the pick-up itself but, most likely, some wakefields also induce a significant amount of signal in the pick-up. When electron bunches travel in the beam pipe, various waveguide modes may be excited along their path and then propagate together with the bunch train. Since these modes can be produced at many locations in the ring and since they propagate with different velocities, some may be detected at the same time as the bunch train (in that case, the wakefields induce aperiodic ringing between the signals produced by the bunches), while others may arrive at the pick-up location up to tens of ns after the passage of the bunch train.

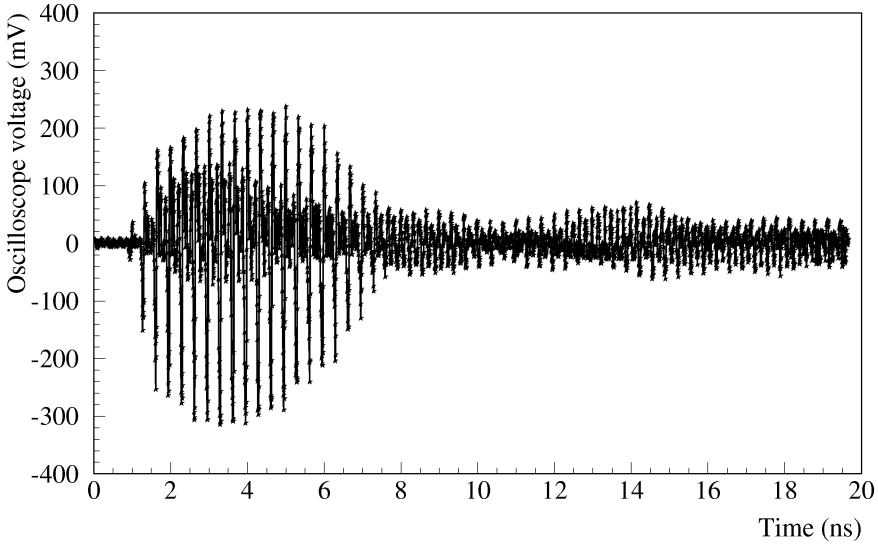

Figure 16: Time structure of the signal induced in the pick-up by the passage of one bunch train in the CTF3 isochronous ring. The 6-7 ns long pulse is clearly visible on the left-hand side, while some signal induced by the wakefields can be observed on the right-hand side.

The same measurement was then performed with a different timing of the streak camera trigger, in order to visualize the waveform obtained after the bunch frequency multiplication with a factor five. Figure 17 shows how the bunch trains are interleaved to form a pulse with a bunch spacing about five times smaller than in the original pulse (the precision of our measurement does not allow a very accurate determination of the distance between the bunches).

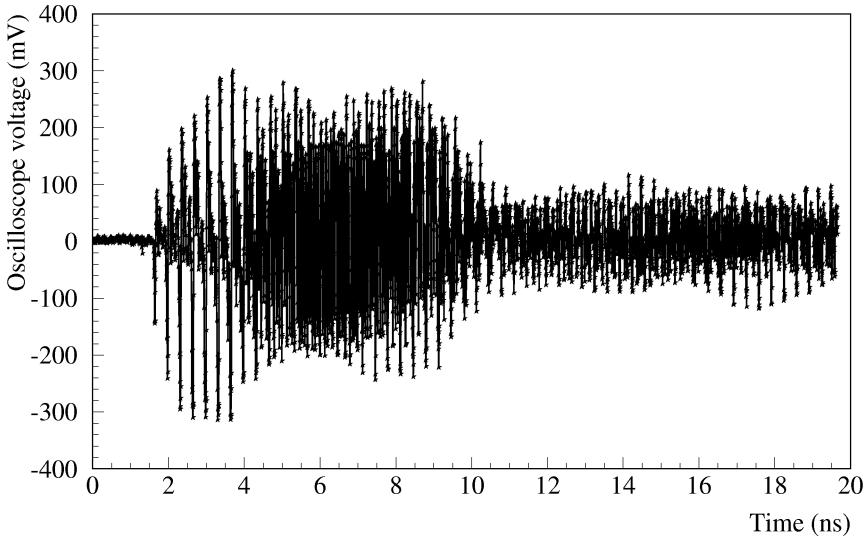

Figure 17: Same as Figure 16, but after combination of five bunch trains.

Since the source does not deliver identical pulses, variations in length may occur from one bunch train to the other. As a result, the longitudinal overlap between the five bunch trains is not perfect and the bunch frequency multiplication only occurs in the core of the final pulse. Also, the bunch trains may have slightly different orbits and/or transverse sizes because of the betatron oscillations, depending on the number of turns they perform in the ring after their injection. This leads to variations in the amplitude of the transverse fields from one bunch train to the other: in the pulse obtained after the combination process, different bunch trains do not induce the same amount of signal.

The waveform of the pulse was recorded on the sampling oscilloscope at each step of the bunch frequency multiplication process, see the five plots on the left-hand of Figure 18. It was then divided into nine 1 ns long intervals and the discrete Fourier Transform of the time signal was calculated over each of these intervals. As expected, only the harmonics of 3 GHz are found in the frequency spectrum (because of the attenuation in the cables between the pick-up and the oscilloscope, only the frequencies below 15 GHz are measurable). Since the time signal is 1 ns long only, the harmonics have a certain width, but we are only interested in their maximum amplitude $V_{max}(f_i)$, where $f_i = 3, 6, 9, 12$ and 15 GHz. Knowing the transfer function of the SMA cables, of the 6 dB attenuator and of the wideband amplifier, it is then possible to derive the amplitude of each harmonic at the pick-up output, and the associated power $P(f_i)$. The five plots on the right-hand side of Figure 18 show the evolution of the power (in arbitrary units) associated with each harmonic during the bunch train combination.

The power associated with the 15 GHz harmonic clearly increases while the bunch trains are combined. But the distribution of the power between the various harmonics is not uniform along the bunch train. In particular, at the end of the bunch frequency multipli-

cation process, only the core of the pulse has an almost pure 15 GHz structure, while all harmonics of 3 GHz can still be found at the edges of the pulse. The fact that the bunch trains do not perfectly overlap is the main reason for this effect.

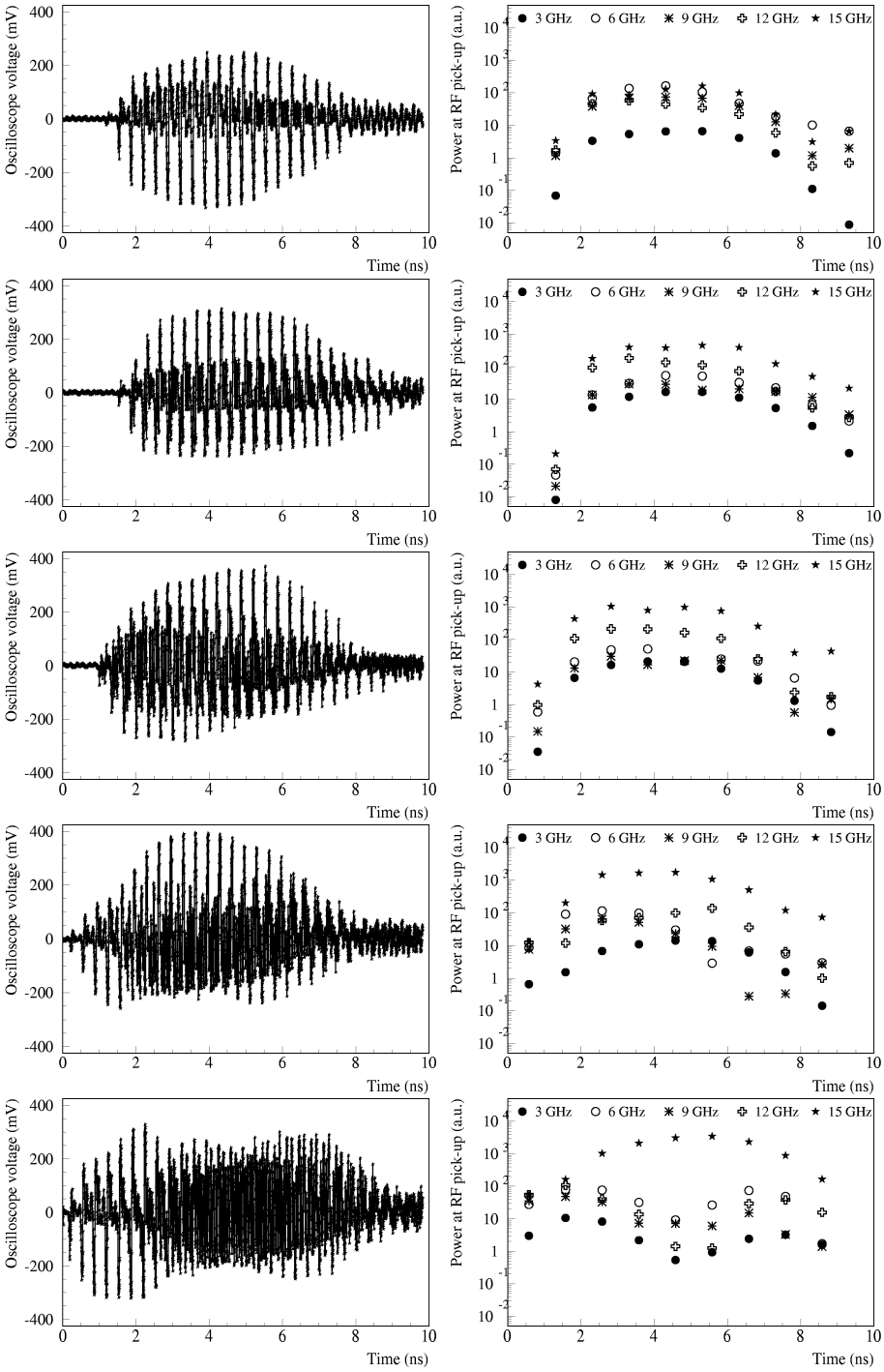

Figure 18: Evolution of the time (left) and frequency (right) structures of the bunch train while the bunch frequency multiplication with a factor five is performed.

A Fourier Transform analysis of the waveforms shown in Figure 16 and 17 was performed. By treating separately the pulse and the tail, we noticed that the power spectrum of the signal induced by the wakefields contains the same harmonics as the signal induced by the bunches themselves, although not with the same amplitudes. For all harmonics, the power found in the first 8 ns of the waveform, i.e. in the pulse, is about one order of magnitude larger than the power found in the last 8 ns of the waveform, i.e. in the tail, see Figure 19. This suggests that, in spite of the presence of wakefields, frequency domain measurements can be performed in order to monitor the bunch frequency multiplication, because the main contribution to the power spectrum of the pulse comes from the bunch train itself. However, the wakefields which travel between the bunches do contribute to the power spectrum as well. Frequency domain measurements do not allow any discrimination between the signal induced by the wakefields and the signal induced by the bunches, which may be a serious limitation when one wants to perform accurate measurements.

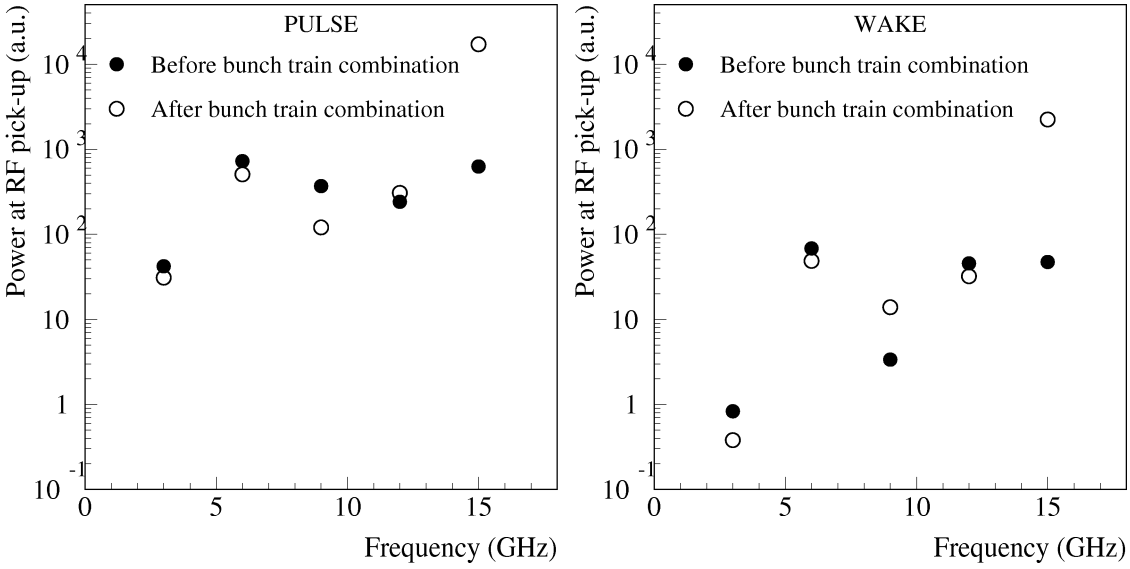

Figure 19: Repartition of the power (in arbitrary units) between various harmonics at the RF pick-up output, before and after the bunch train combination. The left-hand side plot corresponds to the first 8 ns of the signal, while the right-hand side plot corresponds to a 8 ns long time interval in the wake.

5.2 Frequency domain measurements

In order to directly study the evolution of the beam frequency spectrum during the bunch train combination process in the CTF3 isochronous ring, the RF pick-up signal was first filtered in the detection system and then analysed with a fast multi-channel digital oscilloscope in the CTF3 control room.

When performing these measurements, the charge per bunch was found to be about 0.06 nC. The bunch length, measured with a streak camera, was between 7 and 12 ps fwhm (in the following, we consider an average fwhm length of 10 ps). The beam transverse position at the location of the monitor was derived from measurements in two beam position monitors placed upstream and downstream of the RF pick-up: we found respectively -1.0 ± 1.0 mm and -1.6 ± 0.8 mm in the horizontal and vertical directions. MAFIA simulations were performed in order to estimate the power level of the 6.6 ns long pulse at the pick-up output with these experimental conditions, for each harmonic of interest and at each stage of the bunch train combination process, see Table 4. An RF synthetizer driven by a DC pulse generator was then used to inject 6.6 ns long RF signals into the detection system, at each frequency of interest and with the power levels estimated with MAFIA. The output waveforms were stored for further comparison with the signals coming directly from the pick-up.

Step	Power level for each harmonic f_i				
	9 GHz	12 GHz	15 GHz	18 GHz	21 GHz
1	-22.1 dBm	-18.6 dBm	-19.5 dBm	-20.7 dBm	-18.9 dBm
2	-26.3 dBm	-14.4 dBm	-13.5 dBm	-16.5 dBm	-23.1 dBm
3	-26.3 dBm	-14.4 dBm	-10.0 dBm	-16.5 dBm	-23.1 dBm
4	-22.1 dBm	-18.6 dBm	-7.5 dBm	-20.7 dBm	-18.9 dBm
5	-	-	-5.6 dBm	-	-

Table 4: Expected power levels for the harmonics coming from the RF pick-up, at each step of the bunch frequency multiplication with a factor five. The bunch charge is 0.06 nC, the fwhm bunch length is 10 ps and the beam transverse positions are $x = -1.0$ mm and $y = -1.6$ mm.

Figure 20 shows the signals which were extracted from the Uppsala beam monitor and then measured by the oscilloscope at each step of the bunch train combination. The distance between the pulses is 420 ns, which corresponds to the CTF3 isochronous ring circumference, as expected. The signal shape is often distorted because of the contribution of the wakefields. The open circles correspond to the peak amplitude of the output signal obtained when 6.6 ns long RF pulses are injected into the detection system, with the power levels of Table 4. At 15 GHz, the signal amplitude clearly increases each time a new bunch train is injected into the ring and, at the end of the bunch frequency multiplication, most of the power is found in the 15 GHz harmonic, as expected. However, some other channels also receive some signal, but the corresponding pattern is not consistent with a phase error at injection. It is thus probably due to the fact that the longitudinal overlap between the five bunch trains is not perfect (the bunch frequency multiplication mainly occurs in the core of the final pulse). This may also partly explain the discrepancies between the expected and measured signal amplitudes. Another reason for these discrepancies, and for the distorsion of the pulses, may be the presence of wakefields between the bunches (depending on their phase, the wakefields can induce either an increase or a decrease of the output signal amplitude).

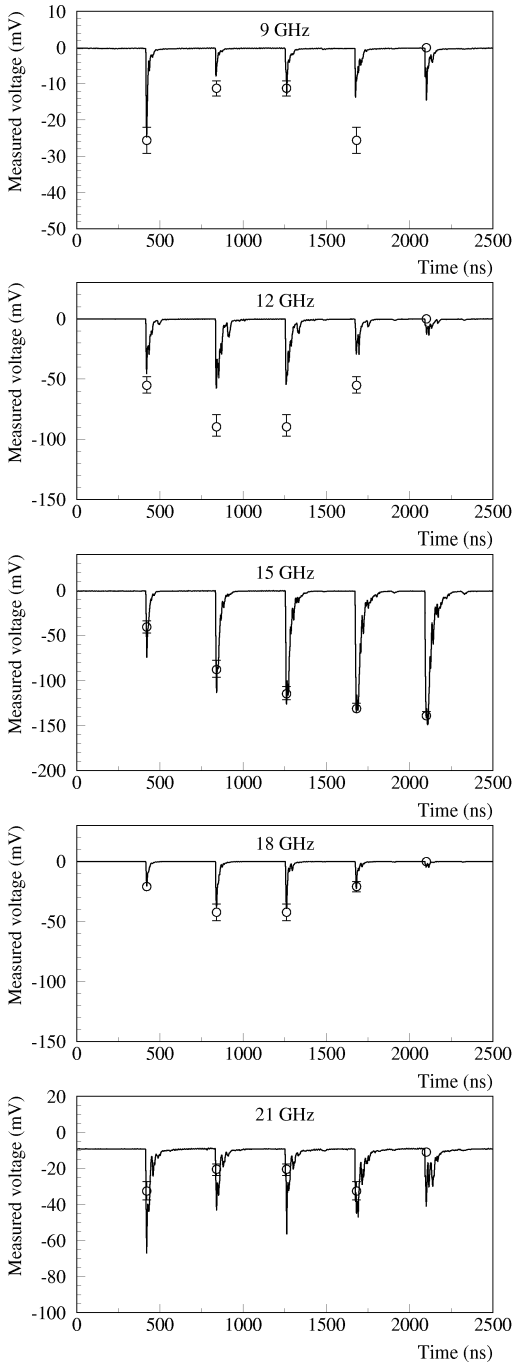

Figure 20: Signals coming from the Uppsala beam monitor, as measured downstream of the instrumentation, while a bunch frequency multiplication with a factor five occurs. The open circles show the expected amplitude for 20 bunches with a charge of 0.06 nC and a fwhm length of 10 ps, travelling at $x = -1.0$ mm and $y = -1.6$ mm. The error bars account for the uncertainties on the measurement of the beam transverse position and of the bunch length.

The same measurement was also performed with a bunch frequency multiplication factor of four and it leads to the same conclusion: the signal amplitude of the 12 GHz channel clearly increases each time a new bunch train is injected into the isochronous ring and, at the end of the bunch frequency multiplication process with a factor four, most of the power is found in the 12 GHz harmonic, as shown in Figure 21.

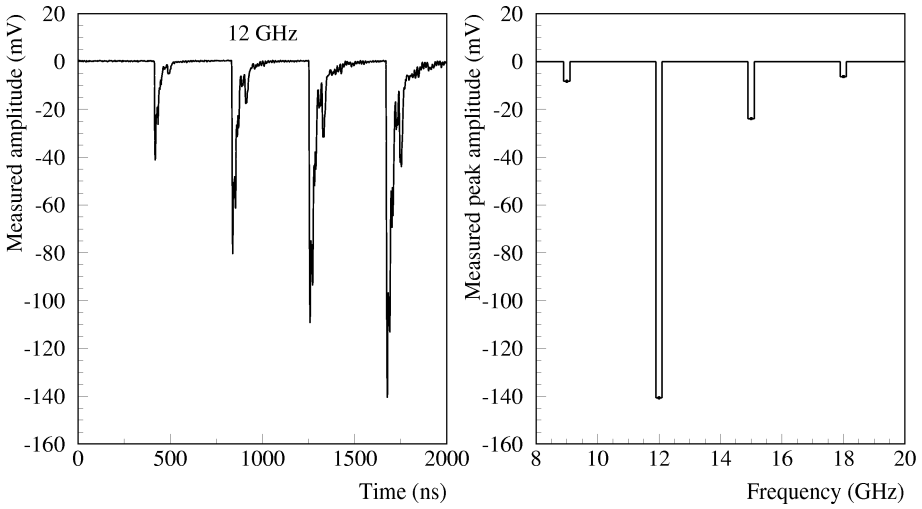

Figure 21: Signals coming from the Uppsala beam monitor, as measured downstream of the 12 GHz channel of the detection system, while a bunch frequency multiplication with a factor four occurs (left), and peak amplitude of the signal detected at the output of each frequency channel at the end of the bunch train combination (right).

6 Conclusion

In this note, we have reported on the successful commissioning of a new instrument aimed at monitoring the combination of electron bunch trains in the isochronous ring of the CTF3 preliminary phase, however with two limitations: the first one is the fact that the time extension of the bunch trains is smaller than the rise time of the read-out electronics, which makes it difficult to measure accurately the absolute power level contained in each harmonic. The second limitation is the presence of waveguide modes propagating in the beam pipe, in the wake of the electron bunches, and leading to a distorsion of the signal coming from the monitor.

In the future stages of the CTF3 project, the length of the bunch trains will be increased and shall reach 140 ns during the bunch frequency multiplication, process which will make the first limitation disappear. However, for a proper and accurate measurement of the power level contained in each harmonic of the CTF3 beam, the parasitic signal due to the waveguide modes propagating in the wake of the bunches should be suppressed.

Acknowledgements

The authors wish to thank G. Geschonke and H. Braun for many fruitful discussions related to this project, E. Jensen for his help with MAFIA simulations, E. Chazarenc for having supervised the fabrication and the installation of the monitor at CERN, E. Butz and D. G-Kurup for their contribution to the detection system tests at Uppsala University, as well as J. Sladen for his help with the time domain measurements.

The research of A. Ferrari has been supported by a Marie Curie Fellowship of the European Community Programme "Improving Human Research Potentiel and the Socio-economic Knowledge Base" under contract number HPMF-CT-2000-00865.

References

[1] R. Corsini (Ed.) et al., "The CLIC RF power source: a novel scheme of two-beam acceleration for electron-positron linear colliders", CERN-99-06 (1999).

[2] R. Corsini, A. Ferrari, L. Rinolfi, T. Risselada, P. Royer and F. Tecker, "Beam dynamics for the CTF3 preliminary phase", CLIC note 470.

[3] R. Corsini, A. Ferrari, L. Rinolfi, P. Royer and F. Tecker, "Report on the second operation period of the CTF3 Preliminary Phase in 2002, 27 May - 23 August", CTF3 note 052, PS/AE note 2002-194.

[4] C. Biscari, R. Corsini, A. Ferrari, A. Gallo, A. Ghigo, L. Rinolfi, P. Royer and F. Tecker, "Report on the third operation period of the CTF3 Preliminary Phase in 2002, 16 September - 25 October", CTF3 note 054, AB note 2003-023.

[5] CST (Computer Simulation Technology), "Mafia Release 4.106", CST Darmstadt, Germany.

[6] A. Ferrari and A. Rydberg, "Design of a bunch phase monitor for the CTF3 preliminary phase", CTF3 note 046, PS/AE note 2002-061.

[7] J. Durand, T. Tardy and R. Trabelsi, "A miniature ultrahigh vacuum feedthrough usable from DC to 20 GHz", PS/LP/96-09 (tech), EST/96-03.

[8] R. Corsini, A. Ferrari, L. Rinolfi, P. Royer and F. Tecker, "Report on the operation of the CTF3 Preliminary Phase, 8 April - 24 May 2002", CTF3 note 049, PS/AE note 2002-141.